Supporting Information

F and Si dual-doping induced oxygen vacancies in $Na_4Fe_3(PO_4)_2P_2O_7$ cathode enables boosting electrochemical performance for sodium storage

Jianhong Gao[ab], Ziwei Chen[ab], Jun Cao[a], Kun Wang[a], Guangxia Tang[c], Ming Zhang[d], Feng Lin[e], Waqar Ahmad[b], Min Ling[a]*, Chengdu Liang[a], and Jun Chen[ab]*

a Zhejiang Provincial Key Laboratory of Advanced Chemical Engineering Manufacture Technology, College of Chemical and Biological Engineering, Zhejiang University, Hangzhou 310027, China.

b Institute of Zhejiang University-Quzhou, Zheda Road 99, Quzhou 324000, China.

c State Key Laboratory of Advanced Chemical Power Sources, Guizhou Meiling Power Sources Co., Ltd., Zunyi, Guizhou 563000, China

d Quzhou Jingzhou Technology Development Co., Ltd.

e College of Chemical and Materials Engineering, Quzhou University, Quzhou, 324000, China

* Corresponding author. E-mail address: minling@zju.edu.cn (Min Ling); qiujinchen@zju.edu.cn (Jun Chen).

1. Experimental Section

1.1 Material synthesis

$Na_4Fe_3(PO_4)_2P_2O_7$ were synthesized via a simple liquid-phase method. All the reagents using in the synthesis were analytical grade. Firstly, stoichiometric ratios of NaH_2PO_4 (99.0% pure, Aladdin), $Fe(NO_3)_3$❿$9H_2O$ (99.9% pure, Aladdin), $C_6H_8O_7 \cdot H_2O$ (99.5% pure, Aladdin) were added into deionized water, and stirred overnight at room temperature. The yellow-green clear solution was then dried in an oven at 150 °C for 1 h to obtain precursor. After grinding, the precursor powder was pre-calcined at 300 °C for 3 h in tube furnace with a heating rate of 5 °C min^{-1}. The obtained powders were further pelletized under 15 MPa and calcined again at 550 °C for 10 h with a heating rate of 5 °C min^{-1} (denoted as NFPP). With adding sodium fluoride (NaF, Aladdin) as F source and silicon acetate ($C_8H_{12}O_8Si$, Aladdin) as Si source, F-doped, Si-doped and F/Si dual-doped NFPP ($Na_{4+x}Fe_3(PO_4)_{2-x}(SiO_4)_xP_2O_7F_y$) were prepared through the same method mentioned above. The exploration of specific doping amount of individual F or Si element was involved to find out the optimal doping amount. Finally, the best dual-anionic-doped $Na_{4+x}Fe_3(PO_4)_{2-x}(SiO_4)_xP_2O_7F_y$ sample and control samples were denoted as NFPP-0.1F/0.05Si (x=0.05, y=0.1), NFPP-0.1F (y=0.1), and NFPP-0.05Si (x=0.05), respectively.

1.2 Material characterization

Field-emission scanning electron microscopy (FESEM) images were collected using Regulus 8230. High-resolution transmission electron microscopy (HRTEM) images, energy dispersive X-ray spectroscopy (EDS) mapping images, and selected area electron diffraction (SAED) pattern were recorded by using a Talos F200X. The measurement of Na/Fe/P stoichiometry was conducted on inductively coupled plasma−atomic emission spectrometry (PE NeXION 5000G). The crystal structure and phase composition of the samples were obtained on a Bruker AXS diffractometer (D8 Advance) using Cu Kα radiation at λ=1.54 Å. GSAS software was used for XRD data analysis. The vibrations of the functional groups were observed using Fourier-transform infrared spectroscopy (FTIR). X-ray photoelectron spectroscopy (XPS) was used to confirm the valence of each element in all samples. Room-temperature electron

paramagnetic resonance (EPR) tests were carried out to identify oxygen vacancy on an EPR spectrometer **(**Bruker E500**)** using a 9.45 GHz X-band with 5.00 G modulation amplitude and a 100 kHz magnetic field modulation. Thermogravimetric analysis (TGA) and Raman spectroscopy were involved to analyze the carbon content and type of carbon structure. Moreover, to study the sodium storage mechanism, a series of ex-situ characterizations (ex-situ XRD, ex-situ XPS, and ex-situ EPR) were carried out on electrodes. The electrodes were charged/discharged under 0.1 C (1 C=129 mAh g^{-1}) until stabilizing at specific voltage platforms.

1.3 Electrochemical measurements

Na half cells and full cells were assembled in an argon-filled glove box for further electrochemical measurements. The slurry, which was composed of 70 wt.% active material, 20 wt.% acetylene black and 10 wt.% poly-vinylidene fluoride (dissolved in N-methyl-2-pyrrolidone), was casted on Al foil to obtain cathodes. Na metal foil was adopted as counter electrode in Na half cells. For anodes in Na full cells, 70 wt.% of hard carbon, 20 wt.% acetylene black and 10 wt.% polyvinylidene fluoride (dissolved in N-methyl-2-pyrrolidone) were mixed together and casted on Al foil. All electrodes were dried at 80 ℃ overnight in a vacuum and then cut into 10 mm disks. 1 M $NaClO_4$ dissolved in PC with 5 vol% FEC was used as electrolyte, and Whatman GF/D was used as separator. All cells were aged for 10 h before testing. Electrochemical performance and GITT measurements were studied on Neware battery testing system at 25 ℃. All the half cells were pre-activated under a small rate of 0.1 C for 3 cycles and then tested under different rates in the rest cycles. Electrochemical Impedance Spectroscopy (EIS) tests and Cyclic voltammetry (CV) tests were performed on CHI600E electrochemical workstation. The electrochemical impedance spectroscopy (EIS) was measured under a frequency region of 0.01 Hz to 1×10^5 Hz with a voltage amplitude of 5 mV. CV tests were measured at different scanning rates of 0.1, 0.2, 0.4, 0.6, 0.8, 1.0 mV s^{-1}, respectively. The GITT tests were carried out at 0.05 C with the pulse time of 30 min and followed by a relaxation period of 120 min. The diffusion coefficient (D_{Na+}) can be calculated from the GITT profiles using Fick's second law [1,2]:

$$D_{Na+} = \frac{4}{\pi\tau}\left(\frac{m_B V_m}{M_B S}\right)^2\left(\frac{\Delta E_s}{\Delta E_\tau}\right)^2$$

where τ is the current pulse time; m_B, M_B, and V_m correspond to the mass, molar mass, and molar volume of the active material, respectively; S is the geometric area of the electrode; ΔE_S and ΔE_τ are the potential difference during the open circuit period and the potential change during a constant current pulse excluding the IR drop, respectively.

1.4 DFT calculation

All calculations in this study were performed with the Vienna ab initio Simulation Package (VASP) within the frame of density functional theory (DFT) [3–5]. The exchange-correlation interactions of electron were described via the generalized gradient approximation (GGA) with PBE functional, and the projector augmented wave (PAW) method was used to describe the interactions of electron and ion [6,7]. Additionally, the DFT-D3 method was used to account for the long-range van der Waals forces present within the system and the DFT+U method was used for the description of d electrons of Fe [8]. The Monkhorst-Pack scheme was used for the integration in the irreducible Brillouin zone. The kinetic energy cut-off of 450 eV was chosen for the plane wave expansion. The lattice parameters and ionic position were fully relaxed, and the total energy was converged within 10^{-5} eV per formula unit. The final forces on all ions are less than 0.02 $Å^{-1}$. For the calculation of Na^+ migration, the CINEB method was employed.

Table S1. XRD Rietveld refinement results of NFPP.

Atom	x	y	z	Occ.	Iso.
Na1	0.007964	0.477807	0.334332	0.9543	0.02500
Na2	0.032933	0.044526	0.487179	0.9994	0.03885
Na3	0.201214	0.224058	0.374319	0.9518	0.03484
Na4	0.393154	0.241438	0.230936	0.9639	0.01576
Fe1	0.132806	0.494709	0.077564	0.9449	0.03786
Fe2	0.162740	0.010051	0.090327	1.0000	0.03526
Fe3	0.240853	0.744652	0.344680	0.9813	0.00773
P1	0.048750	0.233178	0.040947	0.9593	0.02992
P2	0.057967	0.758633	0.207642	1.0000	0.08872
P3	0.179439	0.480864	0.587750	1.0000	0.01022
P4	0.291446	0.506806	0.055350	1.0000	0.06516
O1	0.000000	0.150335	0.203096	1.0000	0.02500
O2	0.009342	0.233475	0.774608	0.9999	0.00584
O3	0.026123	0.367733	0.105446	1.0000	0.02500
O4	0.042174	0.612302	0.103328	1.0000	0.01671
O5	0.122024	0.763445	0.374766	1.0000	0.11208
O6	0.127611	0.223065	0.000923	1.0000	0.05114
O7	0.114075	0.423760	0.380011	0.7774	0.15322
O8	0.150567	0.046919	0.407848	1.0000	0.11116
O9	0.235820	0.412763	0.614743	1.0000	0.57364
O10	0.252270	0.597089	0.112004	1.0000	0.01133
O11	0.246385	0.370125	0.059641	1.0000	0.00136
O12	0.269218	0.116764	0.036574	1.0000	0.00298
O13	0.358077	0.463381	0.263913	1.0000	0.02500
O14	0.379858	0.035428	0.262517	0.9935	0.03974
O15	0.406960	0.377225	0.600540	1.0000	0.01891

Table S2. XRD Rietveld refinement results of NFPP-0.1F.

Atom	x	y	z	Occ.	Iso.
Na1	0.001758	0.478034	0.352608	1.0000	0.02500
Na2	0.035938	0.041516	0.491298	1.0000	0.04186
Na3	0.204500	0.247200	0.319400	0.9774	0.02480
Na4	0.394100	0.263500	0.243300	1.0000	0.02500
Fe1	0.138086	0.507582	0.075999	0.9903	0.02100
Fe2	0.163750	0.001363	0.087011	0.9991	0.02811
Fe3	0.242901	0.746028	0.340068	0.9800	0.01226
P1	0.052159	0.234447	0.041269	1.0000	0.03440
P2	0.063858	0.756463	0.209262	1.0000	0.04658
P3	0.180700	0.487496	0.591078	0.9985	0.01115
P4	0.298788	0.501684	0.063288	0.9611	0.05916
O1	0.000000	0.151595	0.208546	1.0000	0.02500
O2	0.014420	0.203628	0.792826	0.9967	0.05142
O3	0.040617	0.368821	0.073960	1.0000	0.02634
O4	0.054176	0.639734	0.104786	1.0000	0.02500
O5	0.117852	0.765305	0.381983	1.0000	0.06184
O6	0.122732	0.192353	0.014292	1.0000	0.08459
O7	0.133398	0.446819	0.397179	1.0000	0.02500
O8	0.156115	0.040892	0.392298	1.0000	0.02500
O9	0.228035	0.383480	0.609006	1.0000	0.02613
O10	0.234874	0.610428	0.104294	1.0000	0.02500
O11	0.245627	0.390401	0.039343	1.0000	0.00841
O12	0.273127	0.107104	0.055160	1.0000	0.02500
O13	0.350056	0.470455	0.258506	1.0000	0.02500
O14	0.371156	0.024414	0.258506	1.0000	0.02500
O15	0.412540	0.368475	0.579094	1.0000	0.02500
F1	0.024936	0.020623	0.017290	0.1000	0.02500

Table S3. XRD Rietveld refinement results of NFPP-0.05Si.

Atom	x	y	z	Occ.	Iso.
Na1	0.008352	0.466122	0.329478	1.0000	0.02500
Na2	0.044057	0.050916	0.484553	1.0000	0.02500
Na3	0.203377	0.211204	0.344446	1.0000	0.02432
Na4	0.396122	0.251801	0.237956	1.0000	0.02500
Fe1	0.131114	0.519639	0.078494	0.9384	0.02500
Fe2	0.158993	0.002828	0.055730	0.9840	0.02500
Fe3	0.231573	0.747020	0.353743	0.9581	0.02500
P1	0.047719	0.236450	0.013334	0.9973	0.02500
P2	0.054214	0.782638	0.218520	0.9875	0.02500
P3	0.171046	0.483088	0.560815	0.9875	0.02500
P4	0.302322	0.509229	0.067401	0.9875	0.02500
O1	0.009600	0.147500	0.174600	1.0000	0.02500
O2	0.013000	0.197800	0.801800	1.0000	0.02500
O3	0.043400	0.369400	0.059500	1.0000	0.02500
O4	0.057500	0.637200	0.104800	1.0000	0.02500
O5	0.122200	0.757000	0.391000	1.0000	0.02500
O6	0.131300	0.188900	0.000000	1.0000	0.02500
O7	0.135100	0.457300	0.388500	1.0000	0.02500
O8	0.161900	0.035100	0.383000	1.0000	0.02500
O9	0.234000	0.374300	0.616600	1.0000	0.02500
O10	0.236200	0.611800	0.111100	1.0000	0.02500
O11	0.240300	0.385500	0.042800	1.0000	0.02500
O12	0.268000	0.103100	0.057700	1.0000	0.02500
O13	0.344000	0.476400	0.251700	1.0000	0.02500
O14	0.373000	0.012200	0.263300	1.0000	0.02500
O15	0.416100	0.369700	0.565600	1.0000	0.02500
Si1	0.113246	0.613993	0.021433	0.0125	0.02500

Si2	0.054214	0.782638	0.218520	0.0125	0.02500
Si3	0.171046	0.473088	0.560815	0.0125	0.02500
Si4	0.302322	0.509229	0.067401	0.0125	0.02500

Table S4. XRD Rietveld refinement results of NFPP-0.1F/0.05Si.

Atom	**x**	**y**	**z**	**Occ.**	**Iso.**
Na1	0.009637	0.473133	0.352725	1.0000	0.02500
Na2	0.035659	0.078196	0.494532	1.0000	0.02500
Na3	0.201361	0.263824	0.356947	1.0000	0.02500
Na4	0.411943	0.254953	0.237064	1.0000	0.02500
Fe1	0.126760	0.524736	0.035429	0.9220	0.02500
Fe2	0.158536	0.000360	0.075650	0.9399	0.02500
Fe3	0.241793	0.747081	0.347082	0.9523	0.02500
P1	0.051400	0.227500	0.024500	0.9875	0.02500
P2	0.068000	0.763200	0.216000	0.9875	0.02500
P3	0.179100	0.486400	0.583300	0.9875	0.02500
P4	0.292500	0.501500	0.072900	0.9875	0.02500
O1	0.009600	0.147500	0.174600	1.0000	0.02500
O2	0.013000	0.197800	0.801800	1.0000	0.02500
O3	0.043400	0.369400	0.059500	1.0000	0.02500
O4	0.057500	0.637200	0.104800	1.0000	0.02500
O5	0.122200	0.757000	0.391000	1.0000	0.02500
O6	0.131300	0.188900	0.000000	1.0000	0.02500
O7	0.135100	0.457300	0.388500	1.0000	0.02500
O8	0.161900	0.035100	0.383000	1.0000	0.02500
O9	0.234000	0.374300	0.616600	1.0000	0.02500
O10	0.236200	0.611800	0.111100	1.0000	0.02500
O11	0.240300	0.385500	0.042800	1.0000	0.02500
O12	0.268000	0.103100	0.057700	1.0000	0.02500

O13	0.344000	0.476400	0.251700	1.0000	0.02500
O14	0.373000	0.012200	0.263300	1.0000	0.02500
O15	0.416100	0.369700	0.565600	1.0000	0.02500
Si1	0.051400	0.227500	0.024500	0.0116	0.02500
Si2	0.068000	0.763200	0.216000	0.0125	0.02500
Si3	0.179100	0.486400	0.583300	0.0125	0.02500
Si4	0.292500	0.501500	0.072900	0.0125	0.02500
F1	0.268000	0.103100	0.057700	0.1000	0.02500

Table S5. The lattice parameters of as-prepared samples.

Material	**a [Å]**	**b [Å]**	**c [Å]**	**V [Å^3]**
NFPP	9.658	10.941	12.256	564.26
NFPP-0.1F	9.666	10.939	12.284	566.37
NFPP-0.05Si	9.776	10.928	12.262	566.43
NFPP-0.1F/0.05Si	9.810	10.930	12.250	570.04

Table S6. ICP results.

mass ratio	**Na**	**Fe**	**P**
NFPP	1.24	2.24	1.62
NFPP-0.1F	1.37	2.45	1.80
NFPP-0.05Si	1.16	2.10	1.53
NFPP-0.1F/0.05Si	1.16	2.07	1.50

Table S7. Fe^{3+}/Fe^{2+} redox couples and corresponding peak-to-peak separation

sample	**Na1 (V)**		**Na4 (V)**		**ΔV1**	**ΔV4**
	oxidation	reduction	oxidation	reduction		
NFPP	3.01	2.85	3.26	3.18	0.16	0.08
NFPP-0.1F	3.02	2.82	3.25	3.19	0.20	0.06
NFPP-0.05Si	3.02	2.84	3.25	3.18	0.18	0.07

NFPP-0.1F/0.05Si	2.99	2.86	3.25	3.19	0.13	0.06

Table S8 The lattice parameters of NFPP-0.1F/0.05Si at different voltage during the initial charge/discharge process in ex-situ XRD test.

Material	**a [Å]**	**b [Å]**	**c [Å]**	**V [Å^3]**
pristine	18.037	6.524	10.532	1239.34
Charge to 2.8 V	17.985	6.514	10.519	1232.38
Charge to 3.0 V	17.946	6.512	10.460	1222.42
Charge to 3.2 V	17.976	6.511	10.463	1224.61
Charge to 3.6 V	18.046	6.533	10.536	1227.14
Charge to 4.0 V	17.929	6.520	10.471	1223.91
Charge to 4.4 V	17.909	6.511	10.469	1220.68
Discharge to 4.0 V	17.985	6.507	10.459	1224.15
Discharge to 3.6 V	17.972	6.519	10.482	1228.05
Discharge to 3.2 V	17.908	6.521	10.484	1224.38
Discharge to 2.8 V	17.997	6.510	10.453	1224.69
Discharge to 2.4 V	17.954	6.505	10.473	1223.22
Discharge to 1.4 V	17.955	6.520	10.485	1227.54

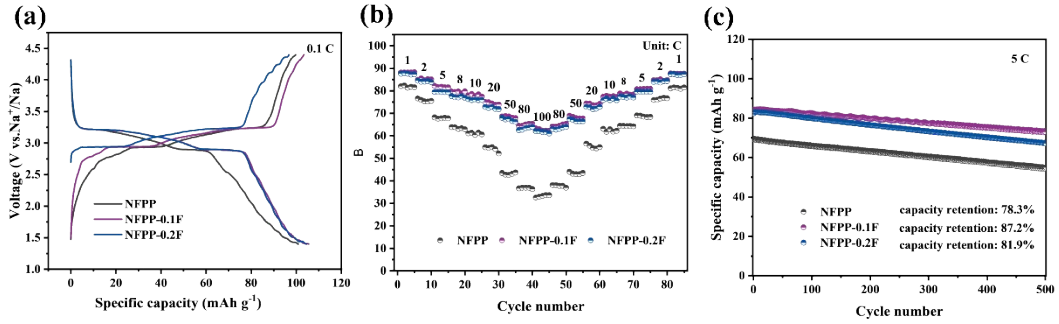

Figure S1. The electrochemical performance of different amount of F doped NFPP. (a) Initial charge/discharge profile at 0.1C; (b) Rate performance from 1 C to 100 C; (c) Long cycle performance at 5 C.

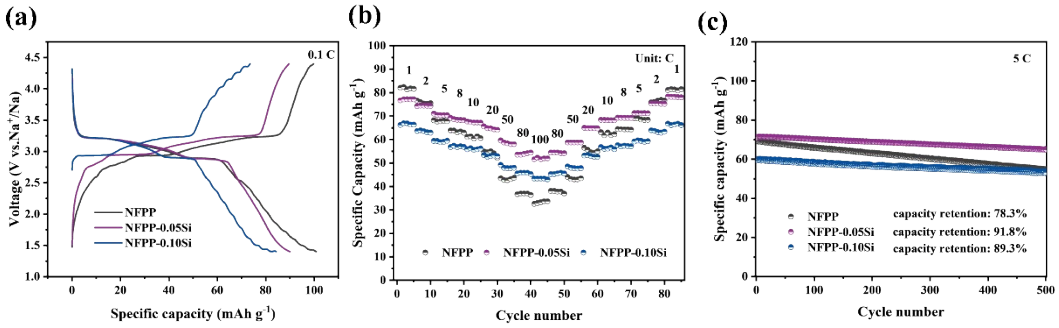

Figure S2. The electrochemical performance of different amount of Si doped NFPP. (a) Initial charge/discharge profile at 0.1C; (b) Rate performance from 1 C to 100 C; (c) Long cycle performance at 5 C.

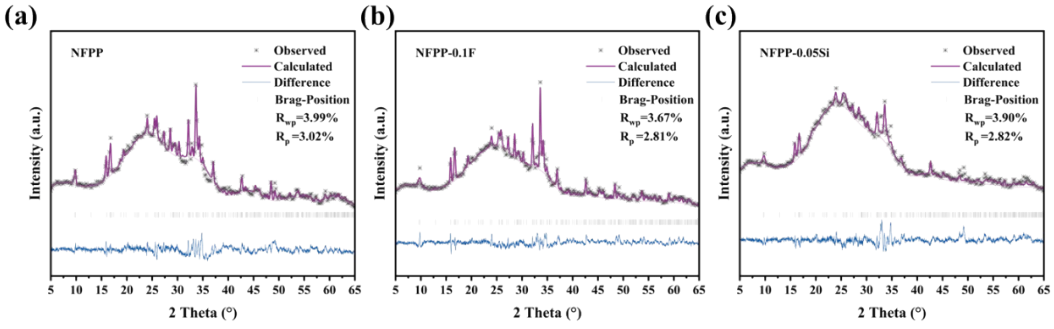

Figure S3. Rietveld refinement results of XRD patterns: (a) NFPP; (b) NFPP-0.1F; (C) NFPP-0.05Si.

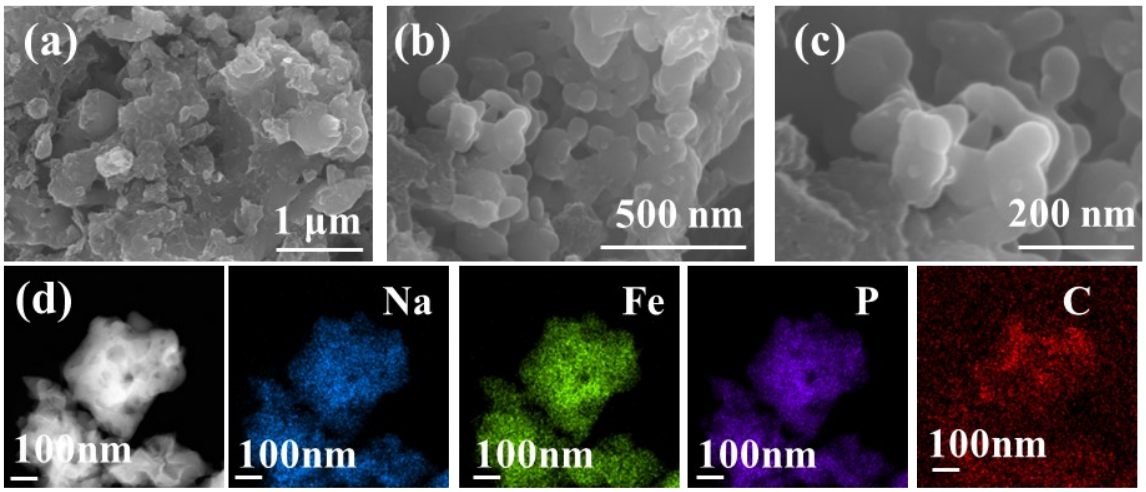

Figure S4. The morphology and elemental distribution of NFPP. (a-c) SEM images with different magnifications; (d) EDS elemental mapping images.

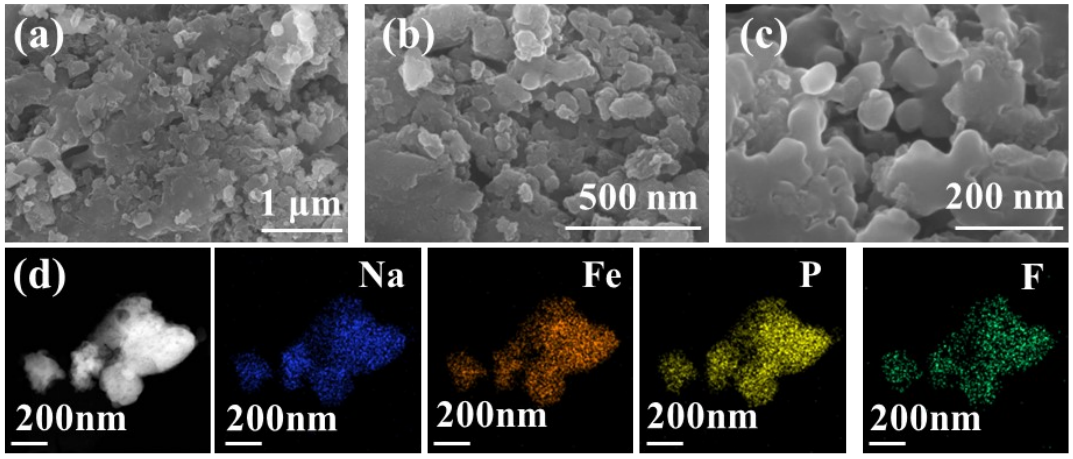

Figure S5. The morphology and elemental distribution of NFPP-0.1F. (a-c) SEM images with different magnifications; (d) EDS elemental mapping images.

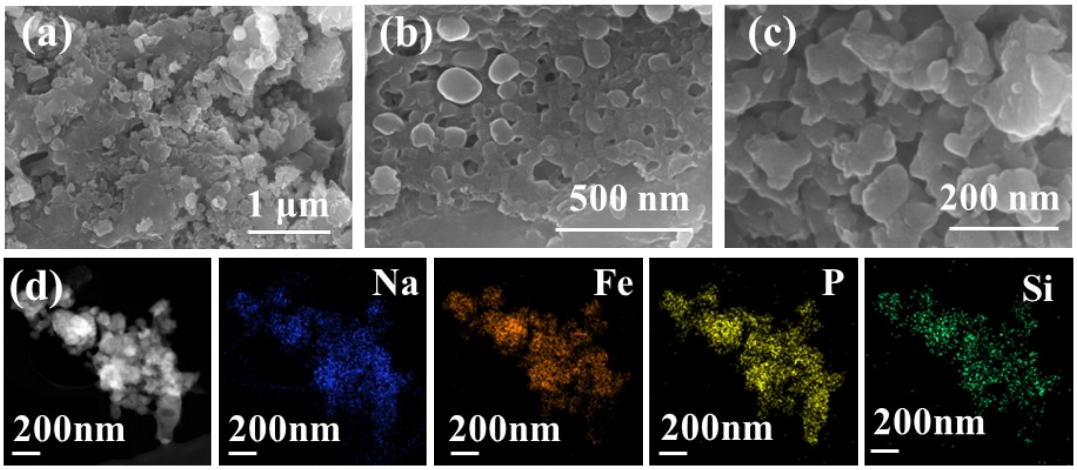

Figure S6. The morphology and elemental distribution of NFPP-0.05Si. (a-c) SEM images with different magnifications; (d) EDS elemental mapping images.

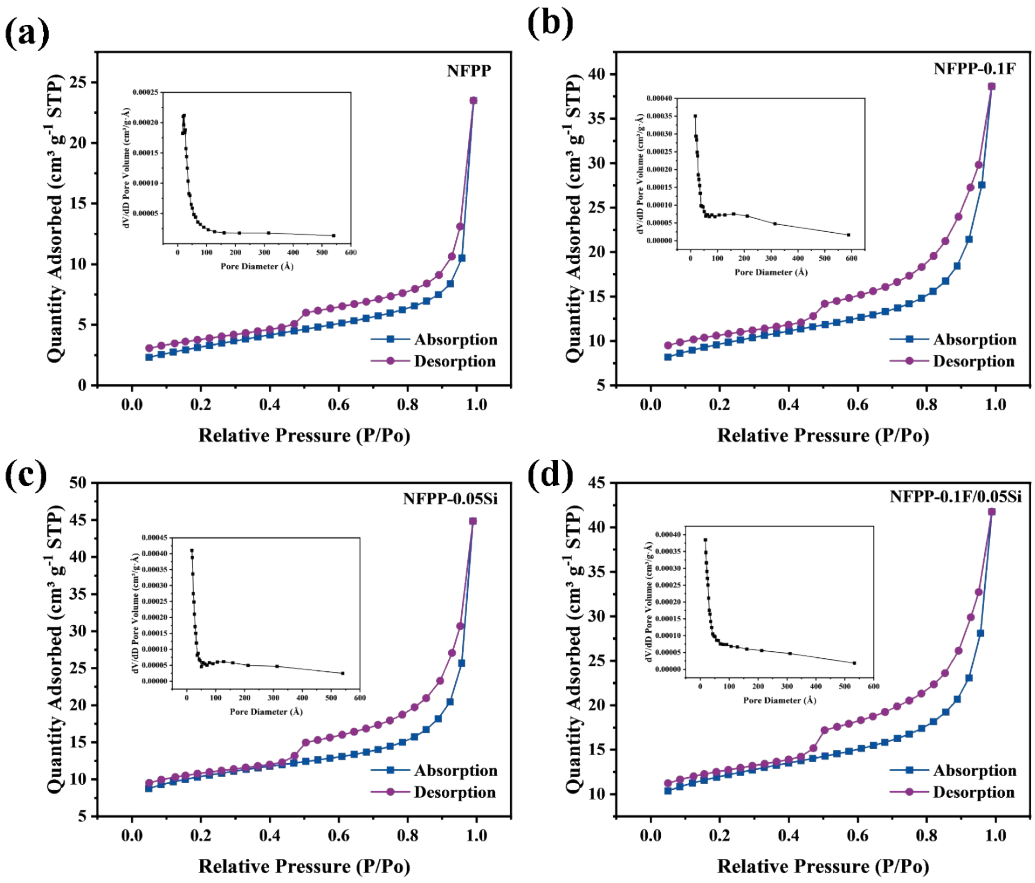

Figure S7. Nitrogen adsorption–desorption isotherm and pore-size distribution.

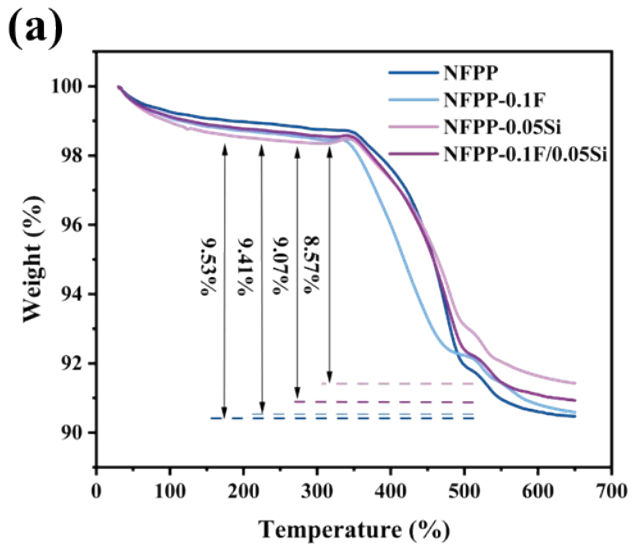

Figure S8. TG curves of all composite samples.

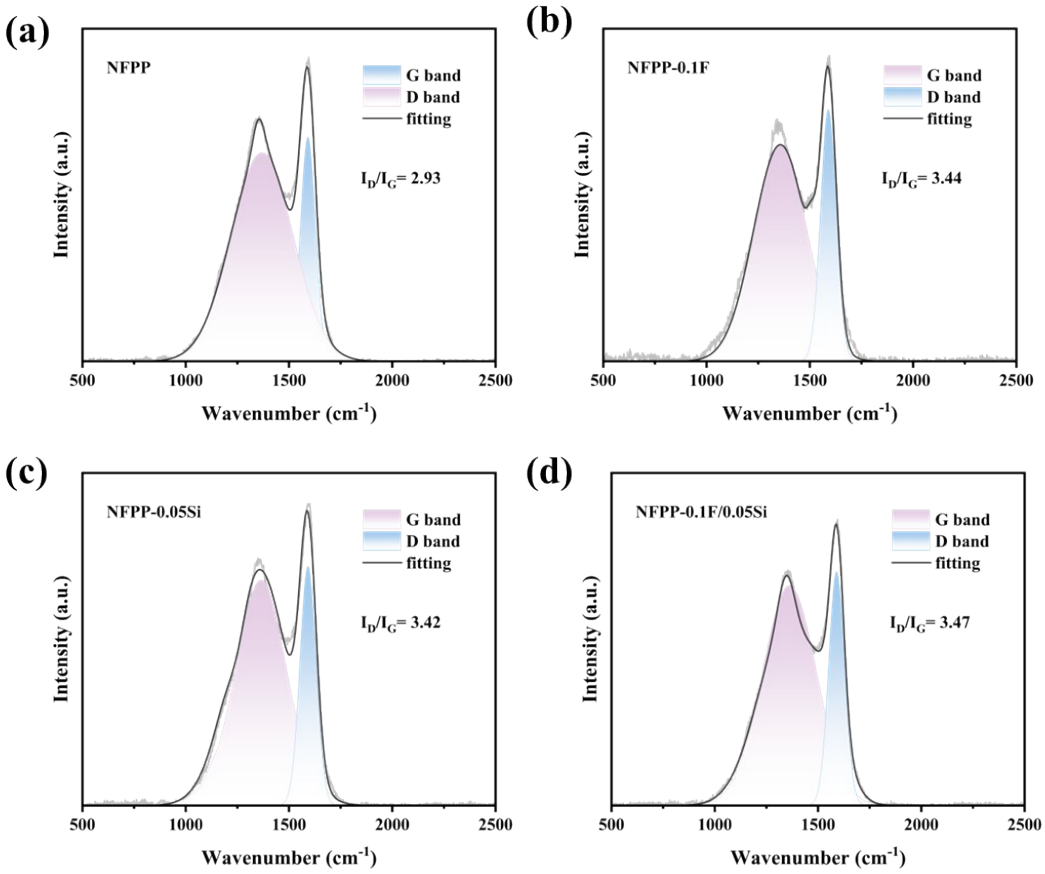

Figure S9. Raman spectrum results: (a) NFPP; (b) NFPP-0.1F; (c) NFPP-0.05Si; (d) NFPP-0.1F/0.05Si.

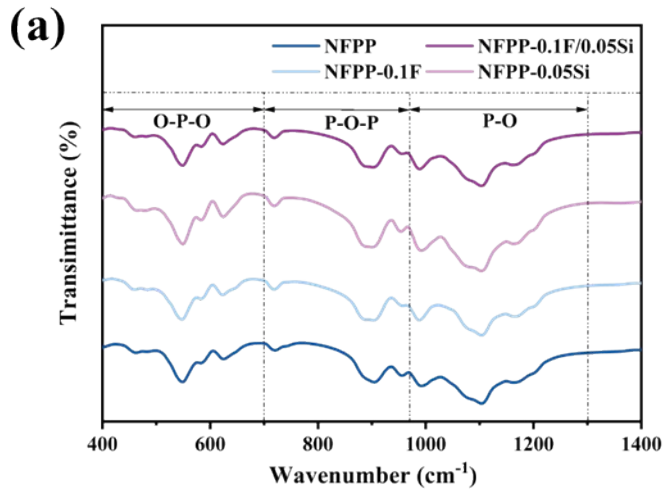

Figure S10. FT-IR spectra of all composite samples.

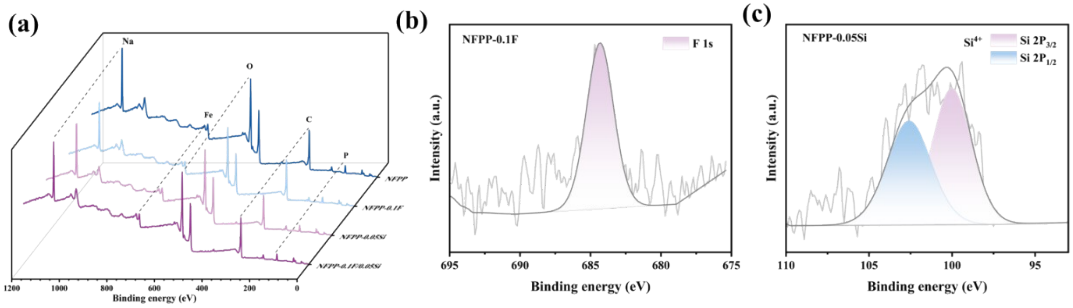

Figure S11. (a) XPS survey spectrum of all composite samples; (b) F 1s in NFPP-0.1F sample; (c) Si 2p in NFPP-0.05Si sample.

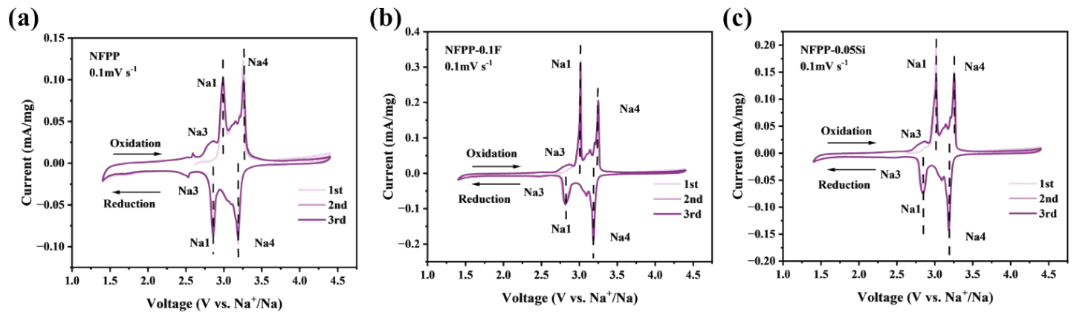

Figure S12. CV curves tested between 1.4-4.4 V at 0.1 mV s^{-1}, respectively. (a) NFPP; (b) NFPP-0.1F; (c) NFPP-0.05Si.

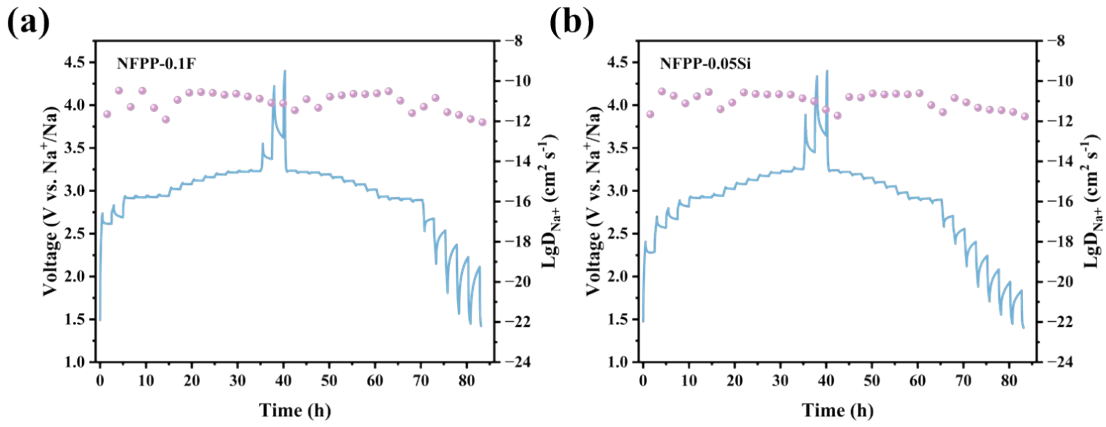

Figure S13. GITT curves and corresponding chemical diffusion coefficient of Na^+ as a function of time calculated: (a) NFPP-0.1F; (b) NFPP-0.05Si.

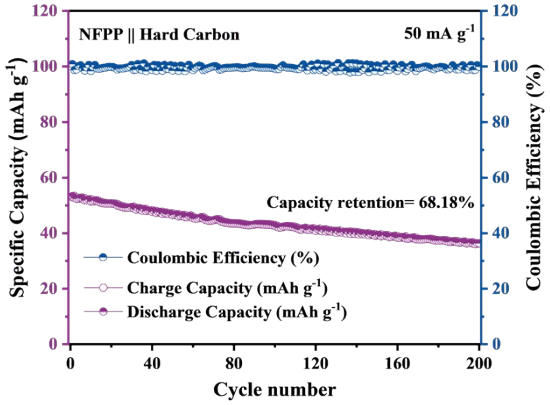

Figure S14. Cycling stability of NFPP||hard carbon full cell at 50 mA g^{-1} for 200 cycles.

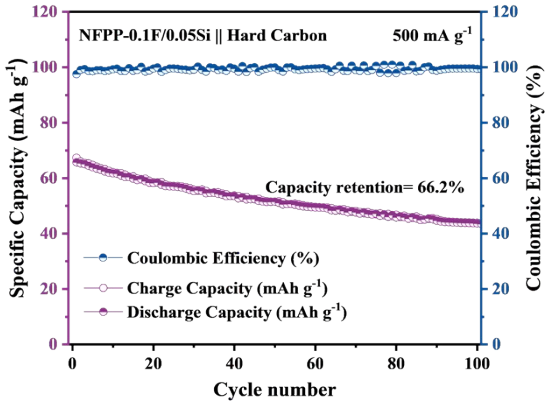

Figure S15. Cycling stability NFPP-0.1F/0.05Si||hard carbon full cell at 500 mA g^{-1} for 100 cycles.

References

1 Y. Liu, N. Zhang, F. Wang, X. Liu, L. Jiao and L. Fan, *Adv Funct Materials*, 2018, **28**, 1801917.

2 X. Ge, H. Li, J. Li, C. Guan, X. Wang, L. He, S. Li, Y. Lai and Z. Zhang, *Small*, 2023, **19**, 2302609.

3 G. Kresse and J. Furthmüller, *Computational Materials Science*, 1996, **6**, 15–50.

4 G. Kresse and J. Furthmüller, *Phys. Rev. B*, 1996, **54**, 11169.

5 J. P. Perdew, K. Burke, M. Ernzerhof, *Phys. Rev. Lett.* 1996, **77**, 3865..

6 S. Maintz, V.L. Deringer, A.L. Tchougréeff and R. Dronskowski, *J. Comput. Chem.*, 2013, **34**, 2557–2567.

7 P. E. Blöchl, *Phys. Rev. B*, 1994, **50**, 17953.

8 G. Kresse and D. Joubert, *Phys. Rev. B*, 1999, **59**, 1758.